Theor Chem Acc (2012) 131:1150
DOI 10.1007/s00214-012-1150-x

REGULAR ARTICLE

On the kinetics and thermodynamics of S–X (X = H, CH_3, SCH_3, $COCH_3$, and CN) cleavage in the formation of self-assembled monolayers of alkylthiols on Au(111)

Madhavan Jaccob · Gopalan Rajaraman · Federico Totti

Received: 14 July 2011 / Accepted: 13 September 2011 / Published online: 18 February 2012

Abstract Abounding potential technological applications is one of the many reasons why adsorption of aliphatic thiols on gold surface is a subject of intense research by many research groups. Understanding and exploring the nature of adsorbed species, the site of adsorption and the nature of interaction between adsorbed species and the gold surface using experimental and theoretical investigations is an active area of pursuit. However, despite a large number of investigations to understand the atomistic structures of thiols on Au(111), some of the basic issues are still unaddressed. For instance, there is still no clear information about the mechanism of adsorption of alkylthiol on gold surface. Furthermore, the reactivity and mechanism of adsorption of alkylthiol is likely to differ when gold adatoms and/or vacancies in the gold layers are considered. In this work, we have tackled these issues by computing the stationary states involved in the thiols adsorption in order to shed light on the kinetics aspects of adsorption process. In this respect, we have considered a variety of thiols into consideration such as methylthiol, dimethylsulfide, dimethyldisulfide, thioacetates, and thiocyanates. We have also considered the cleavage mechanism in the clean and the reconstructed surface scenario and the structure, energetics and spin densities have been computed using electronic structure calculations. For all the studied cases, an homolytic cleavage of CH_3S–X (X = H, CH_3, SCH_3, CN, and $COCH_3$) bond has been found to occur upon adsorption on the gold surface.

Keywords DFT · Thiols · Kinetics and the mechanism of adsorption · Gold surface

1 Introduction

In recent years, tremendous efforts have been put forward to develop the next generation electronic devices based on the organic/inorganic moieties with high conductivity and optical properties layered on gold surface as self-assembled monolayers (SAMs) [1–9]. Adsorption of aliphatic thiols on gold surface is a subject of interest pursuing their potential applications in nanoproduction, spintronics, biological sensoring, magnetic memory banks, etc. [10–15]. These potential applications of SAMs of thiols on gold surface motivate many researchers to explore the nature of adsorbed species, site of adsorption and the nature of interaction between adsorbed species and the gold surface using experimental and theoretical investigations [36–54]. Earlier experimental and theoretical report suggested that the SAMs of methylthiol preferred to adopt a $(\sqrt{3} \times \sqrt{3})R30°$ structure and may manifest c(2 × 4) superstructure upon varying the chain length; the S head group seems to predominately attack the fcc (face-centered cubic) site of Au(111) surface [16–21]. However, the adsorption site is

Dedicated to Professor Vincenzo Barone and published as part of the special collection of articles celebrating his 60th birthday.

Electronic supplementary material The online version of this article (doi:10.1007/s00214-012-1150-x) contains supplementary material, which is available to authorized users.

M. Jaccob · G. Rajaraman (✉)
Department of Chemistry,
Indian Institute of Technology Bombay,
Powai, Mumbai 400076, India
e-mail: rajaraman@chem.iitb.ac.in

F. Totti (✉)
Dipartimento di Chimica, Polo Scientifico,
INSTM Università degli Studi di Firenze,
via della Lastruccia 3, 50019 Sesto fiorentino, Italy
e-mail: federico.totti@unifi.it

still a matter of great controversy as many possibilities have been lately suggested, including a surface reconstruction and presence of defects on the Au(111) surface leading to the presence of Au adatoms and/or vacancies in the surface monolayers [23–32].

For a long time, a combined experimental and DFT methods unequivocally suggested that adsorption on the bridge site is on top of gold atoms slightly shifted to the fcc hollow if defects are not taken into consideration [33–35]. However, in recent years this perception has changed as surmounting experimental and theoretical evidences suggest that a sandwich complex of two thiols and one gold adatom is the most preferred structure for a low concentration coverage as it is evident from the low temperature STMs and DFT calculations [36, 37, 42, 43]. Undoubtedly, among a large varieties of thiols reported, studies on methyl thiols (MeSH) are the most common [22–54]. Despite a large number of investigations to understand the atomistic structures of thiols on Au(111), some of the basic issues are still unaddressed. One of the outstanding issues in this respect is the cleavage of S–H bonds of methylthiol (MeSH) upon adsorption. Based on electrochemical data, Schlenoff et al. [55] reported that the adsorption of alkylthiols on the gold surface occurs exothermically (reaction energy is −5.5 kcal/mol) with evolution of H_2. This was further supported by XPS, Fourier transform infrared (FTIR) spectroscopy, Fourier transform mass spectrometry, electrochemistry, Raman spectroscopy, and theoretical methods [55–68]. More conclusive evidences have been emerged recently on the release of H_2 by the S–H bond cleavage on various 4-nitrophenylthiols during adsorption on gold surface [69]. A very recent DFT study evaluating the thermodynamics of S–H cleavage reveals that the S–H bond preferentially cleaves with formation of H_2 rather than an Au–H species [70]. On the other hand, there are reports contradicting the cleavage of S–H bond, especially at low coverage regime. Such studies, in fact, reveal that the S–H bond is intact on the clean gold surface [63, 71, 72]. Although theoretical studies in general support the homolytic cleavage of S–H bond [73], the conclusion from calculations was derived solely from thermodynamic stability data without addressing the kinetic barrier involved in the S–H cleavage. Since a prohibitive barrier to reach the transition state will naturally eliminate the possibility of the S–H cleavage, the evaluation of the kinetic barrier height for the S–H cleavage is mandatory to prove/disprove the S–H cleavage in SAMs. Here, we aim to address this issue through quantum chemical calculations on model complexes of SAMs of thiols.

Additionally, we have also considered other variants of thiols routinely used in experiments to probe the S–X (X = H, CH_3, SCH_3, CN, and $COCH_3$) bond cleavage in order to compare them with the S–H case. In fact, among the presented cases above, the S–X bond cleavage is still controversial in some cases (X = Me) [74–77] while it has been unequivocally proved to be cleaved in others (X = SCH_3, $COCH_3$ and CN) [78–92]. In the case of dialkylsulfides (CH_3SCH_3), a combined spectroscopic data suggest that there is no cleavage of S–C bond and sulfur interacts with the metal surface through a dative bond during the formation of SAM [74–77]. SAMs formed from dialkylsulfides are in general found to be less stable than those obtained from thiols and disulfides [93–104]. In contrast to this, Porter et al. [103] reported that S–C bond cleavage occurs in organosulfides, resulting the SAMs that are exactly similar to those of disulfides and thiols. On the other hand, Schlenoff et al. [55] reported that based on the coverage measurements, S–C bond cleavage is minimal. At the same time, both experimental and theoretical studies on other alkyl thiols, such as dimethyldisulphide (DMDS), reveal that the S–S bonds cleaves homolytically leaving a MeS· radical to be adsorbed firmly on the surface. The kinetics of such cleavage has been experimentally measured for DMDS indicating activation energy of 65 kJ/mol [105, 106].

In order to overcome the oxidizing ability of alkylethiol under the conditions of air, light, and moisture [86, 107–110], alternative precursors based on the organic thiocyanates [78–84] and alkylthioacetates [85, 86, 88–90, 92, 93, 111, 112] of gold thiolate assemblies have been synthesized. During the chemisorption of alkylthiocyanates on gold surface, Au–S bond is formed through removal of cyano group in the form of $[Au(CN)_2]^-$ via surface-mediated reduction of the thiocyanate [80, 85]. In contrast to the thiocyanates, chemisorption of the thioacetates on the Au(111) surface is believed to be occurring through a polar transition state associated with a markedly slower rate than that observed for the alkylthiols [86, 90].

In this framework, we have recently explored [73] the thermodynamic aspects of methyl and various substituted thiol molecules using periodic mixed Gaussians-plane waves DFT calculations [73–114]. Our calculations suggest that homolytic cleavage is energetically more favorable and reconstructed Au(111) surface models are energetically favored over clean unreconstructed Au(111) surfaces. Computations using TPSS functional [73, 113] clearly indicate that an energetic gain of −42.7 kcal/mol is obtained when chemisorption of $CH_3S^{\cdot}$ occurs on Au(111) surface. Moreover, the dissociative mechanism occurs with an energy of −7.2 kcal/mol when the formation of H_2 molecule during the adsorption process is taken into account. Despite the availability of many experimental and theoretical reports on the thermodynamic aspects of various alkylthiols on reconstructed and clean Au(111) surface, there is no clear information about the mechanism of adsorption of alkylthiol on gold surface. Furthermore, the

reactivity and mechanism of adsorption of alkylthiol is likely to differ when gold adatoms and/or vacancies in the gold layers are considered. Here, we are planning to tackle these issues by computing the transition states of the S–X bond cleavage to shed light on the kinetics aspects of adsorption process. In this respect, we have considered a variety of thiols into consideration such as methylthiol, dimethylsulfide, DMDS, thioacetates, and thiocyanates. We have considered the cleavage mechanism in both clean and reconstructed surface scenario and discussed the structure, energetics, and spin densities using electronic structure calculations. In addition to kinetics, the formation energies for the most stable radical species have also been computed and discussed.

2 Computational details

All the calculations were performed using Jaguar suit of packages [115] with a hybrid B3LYP functional [116, 117] with a LACVP basis set [118–120]. LACVP basis set comprises the LANL2DZ [121–123] basis set for gold and 6–31G basis for other atoms. Considering computational cost in mind in calculating transition states, a single gold layer model of appropriate size varying from 16 to 20 gold atoms was chosen to mimic the monolayer arrangements. Two optimization procedures were attempted: at the first approximation, we have relaxed all the atoms (full optimization acronym as Fopt) and the corresponding transition states have single imaginary frequency that corresponds to a desired reaction coordinate on the potential energy surface. A slight distortion of Au(111) surface is detected in this procedure, and this is much probably due to the lack of more layers on our model systems. Therefore, we have decided to freeze the first layer of gold atoms as expected in SAM arrangement (partial optimization acronym as Popt). The transition state computed using this procedure, however, had multiple imaginary frequencies due to frozen atoms in the coordinates. The transition states in these cases were characterized by first largest negative frequency, and their nature was graphically verified by using Molden software [124]. Additionally, to mimic the surface scenario, we have decided to add point charges to the explicit gold atoms in order to have a three-layer model with total 192 gold atoms (in total, 192 gold point charges have been added to the existing 16 gold atom models). For the computation of the point charges, a periodic calculation using CP2K program [125] was performed. CP2K is a hybrid basis set formalism known as Gaussian and Plane Wave Method (GPW where the Kohn–Sham orbitals are expanded in terms of contracted Gaussian type orbitals (GTO), while an auxiliary plane wave basis set is used to expand the electronic charge density. A double-ζ GTH basis set and their relativistic norm-conserving pseudo potentials (Goedecker, Teter, and Hutter) [126–128] were used in addition to a plane wave basis set with an energy cutoff of 350 Ry. The Mulliken charges computed by this procedure were then taken to pursue computation of transition states with Jaguar suite of programs. Free energy corrections were computed at 298.15 K.

In order to have another and more reliable check of the reliability of the energetics computed using one-layer model, we have compared the reaction energies of the archetypal species MeSH and MeSMe in clean and reconstructed scenario computed using periodic DFT calculations performed with a unit cell containing three layers of gold atoms [75]. The compared results are reported in Table S1. More computational details about these calculations are discussed in Ref. [75]. The computed reaction energies with both approaches give a consistent trend and a pretty constant deviation providing confidence on our computed energetics using the single-layer model.

3 Results and discussion

3.1 Studies on methylthiol

The chemisorption of methylthiol on gold surface has been modeled by a single layer of Au(111) with 16 gold atoms. Table 1 lists the activation energy of S–H cleavage and reaction energy of the adsorption of methylthiol on gold surface obtained using various theoretical approach listed above. The energy values (barrier height, $\Delta G^{\#}$, and reaction energy, ΔG_{r}) were computed using the following equations unless otherwise mentioned,

$$\Delta G^{\#} = G^{\#}(\mathrm{RS}\cdots X - \{\mathrm{Au_{ad}}\}\mathrm{Au}(111)) - G(\mathrm{RSX} - \{\mathrm{Au_{ad}}\}\mathrm{Au}(111))$$

$$\Delta G_r = \left[G(\mathrm{RS}^{\cdot} - \{\mathrm{Au_{ad}}\}\mathrm{Au}(111)) + G\left(\frac{1}{2}X_2\right)\right] - G(\mathrm{RSX} - \{\mathrm{Au_{ad}}\}\mathrm{Au}(111))$$

where $\{\mathrm{Au_{ad}}\}$ indicates the presence of one gold adatom and X = H, CH_3, SCH_3, CN, and $COCH_3$.

Selected structural parameters of the optimized structures reported in Fig. 1 are presented in Table 2. The barrier height, $\Delta G^{\#}$, for homolytic cleavage of methylthiol on gold surface is found to be 45.5 kcal/mol, and the free energy of the reaction, ΔG_{r}, is found to be endothermic by 14.7 kcal/mol. Since all atoms are relaxed, the layer is no longer rigid resulting in a slight deviation from the planar Au(111) surface expected otherwise.

This implicates the shortcoming of the model employed. Being unable to increase the thickness of the gold slab and

Table 1 Activation and reaction energies of the dissociation of MeSH on the clean and reconstructed surface

	Clean surface			Reconstructed surface
	Fopt	Popt	Popt-dimeric	Popt
$\Delta G^{\#}$	45.5	72.6[a]	20.7	55.4
ΔG_r	14.7	10.1	−14.9	0.2

[a] Upon partial charge, the barrier reduces to 42.4 kcal/mol. *Fopt* Full optimization, *Popt* partial optimization, *Popt-dimeric* partial optimization used for the dimeric case

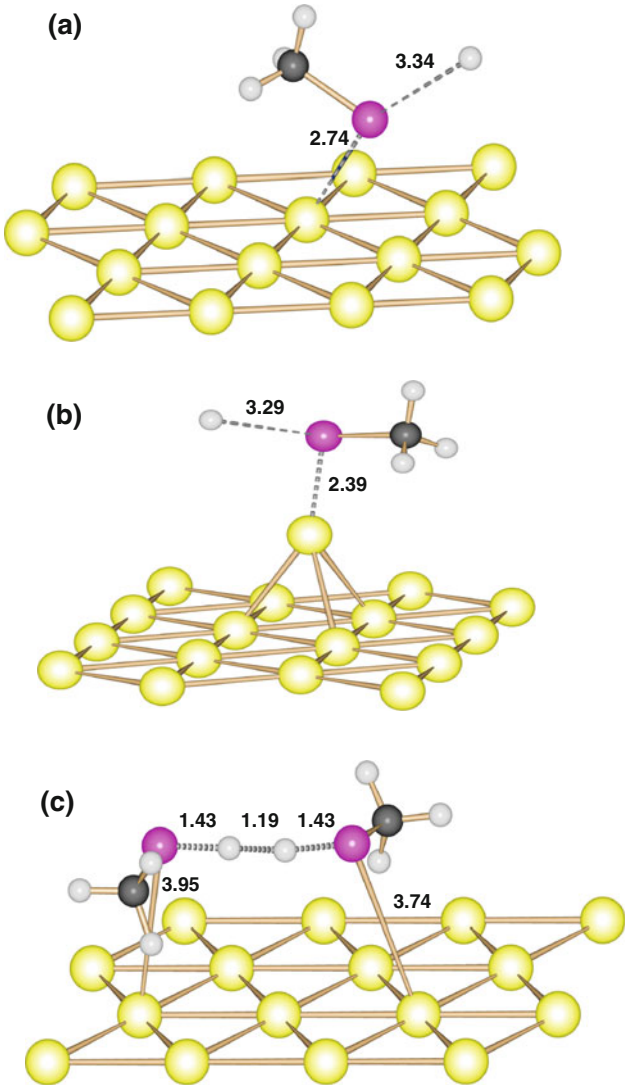

Fig. 1 Computed transition states of MeSH on clean and reconstructed surface (S = pink, H = white, C = gray, Au = yellow)

not expecting a sever surface modification due to strong Au–Au bond, in order to avoid any artificial surface deformation, further calculations were performed by freezing the layered gold atoms.

In this partial optimization of gold surface case, the activation barrier has increased from 45.5 to 72.6 kcal/mol and the reaction energy is computed to be endothermic by 10.1 kcal/mol. The reactant MeSH is adsorbed on the surface with rather a weak Au–S interaction as the sulfur-gold bond lengths are in the range of ~3.5 Å. The sulfur atom sits almost in the middle of an Au triangle in the layer (See Fig. 1) (FCC or HCP hole in SAMs) with all three Au–S bond lengths almost equal in magnitude with a tilt angle ζ of 103.7°. In the transition state, as the S–H bond elongates in a homolytic fashion, sulfur gains significant spin density leading to a stronger Au–S interaction (Fig. 2). This is evident from the shorter Au–S bond lengths detected in the transition state structure with 2.74, 2.87, and 3.08 Å as the nearest Au–S interaction. The tilt angle with respect to the methyl group is found to 121.1°, which is larger than that observed in the reactant. It is important to note here that the tilt angle ζ can be seen as an index of the electron delocalization of the adsorbate on the Au(111) [129]. The S–H bond then cleaves leading to the generation of MeS$^{\cdot}$, which adsorbed firmly on the surface with a much shorter Au–S bond length.

The sulfur atom as product moves rather to a bridge position with the two Au–S bond lengths of 2.815 and 2.900 Å. The homolytic cleavage of the S–H bond is also evident from the abundant spin density of opposite sign detected in the transition state for the sulfur and hydrogen atoms (Fig. 2). Further, calculations performed using the point charges model reduces the barrier to 42.4 kcal/mol compared with 72.6 kcal/mol obtained without the addition of the point charges. The reduction in barrier height is therefore expected as this introduces an electrostatic stabilization of the transition state. Such a large reduction in the barrier height by the addition of point charges reveals that a more realistic model employing several layers of gold atoms or point charges is expected to reduce the barrier height significantly and yield more realistic barrier heights for the reaction to occur at normal conditions. The point charge calculations have been performed only on one model complex, but we believe the relative reduction in the barrier heights to remain approximately the same among different thiols computed here (see below) as also suggested by comparing the reaction energies with more complex models (see Table S1). The S–H bond length is found to be 1.38 Å in the reactant while it elongates in the transition state up to 3.75 Å.

The reactivity and adsorption phenomena is expected to differ when Au adatoms and/or vacancies are present in the top layer of the Au(111). It is evidenced from the reported theoretical and experimental results that the presence of surface gold adatom leads to stabilization of different species in SAMs compared to what is known from the unreconstructed surface scenario. A large number of recent

Table 2 Selected structural parameters of adsorption and dissociation of methyl thiol on clean and reconstructed surface along with spin densities and Mulliken charges (parenthesis) on S and H atoms

	Spin densities		Structural parameters		
	S	H	S–H	Au–S	Au–S–C
Popt					
R	0.0 (0.13)	0.0 (0.07)	1.37	3.54	103.7
TS	0.26 (0.29)	−0.97 (0.02)	3.34	2.74	121.1
$Popt_{dimeric}$					
R	0.0	0.0	1.37	3.34	99.3 (107.3)[a]
TS	0.0 (0.16)	0.0 (−0.07)	1.43	3.74	87.5 (77.6)[a]
$Popt_{Add}$					
R	0.003 (0.21)	0.0 (0.14)	1.38	2.51	99.9
TS	−0.23 (0.23)	0.95 (0.03)	3.28	2.38	102.7
$Popt_{partial\ charge}$					
R	0.0 (0.16)	0.0 (0.09)	1.38	3.20	118.6
TS	−0.01 (0.40)	0.0 (0.21)	3.75	2.51	98.8

[a] Au–S_2–C bond angle, *Fopt* Full optimization, *Popt* partial optimization, *Popt-dimeric* partial optimization used for dimeric case

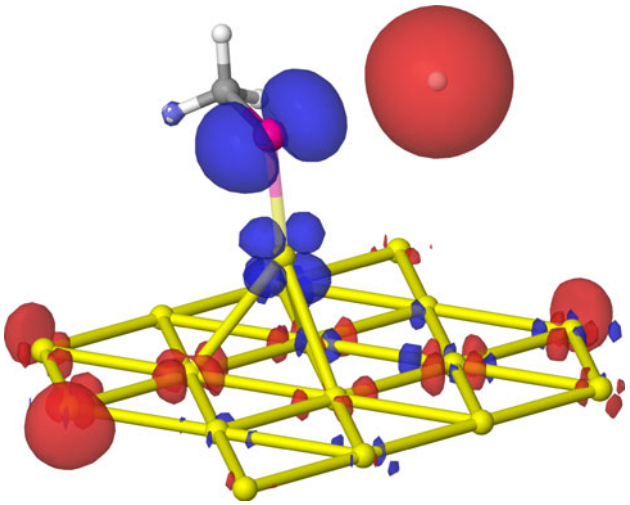

Fig. 2 DFT computed spin density plot of adatom transition state of methyl thiol species on reconstructed surface (S = pink, H = white, C = gray, Au = yellow)

literature supports a reconstructed surface as the most likely model for the SAMs. Therefore, presence of Au adatoms has been taken into consideration for the S–H cleavage. Since we are interested in kinetics of various alkanethiol chemisorption on gold surface, the formation of adatom/vacancies has not been taken into account as this requires much larger models for the computation. The formation of add atom/vacancies has been computed using more realistic three-layer model using periodic DFT methods, and the results are summarized elsewhere [75] (e.g., adatom formation is found to be exothermic by 3.3 kcal/mol). The optimized geometry of the transition states of the methyl thiols on the reconstructed surface is shown in Fig. 1b. Computation yields a barrier height of 55.4 kcal/mol for the S–H cleavage, and the reaction is thermo neutral. Presence of Au adatom substantially lowers the barrier by 17.2 kcal/mol, and the excessive endothermicity observed is brought down to thermonetural conditions. The MeSH in the reconstructed surface prefers a quasi-atop configuration with a tilt angle of 99.9° with Au–S bond length of 2.52 Å. However, the Au–S bond strengthens in the transition state as it gets reduced to 2.39 Å with a tilt angle of 102.8°. The S–H bond elongates to 3.28 Å compared to 1.38 Å observed at the reactant, instead. Moreover, the sulfur prefers a perfect atop configuration. A lower energy barrier in the presence of Au adatom reveals that the defects present in the surface likely to speed up the cleavage process and aid firm chemisorption and ordered SAMs. It has to be noted here that the barrier height might get reduced further upon the addition of point charges as in the unreconstructed scenario discussed earlier.

Although the reactions computed so far are endothermic, it is worth to mention that ΔG_r values have been computed from the adsorbed methyl thiol species. Since the adsorption of thiols on Au(111) is found to be exothermic in nature, the reaction energy from the Au(111) and free reactant is likely to be exothermic. To check this argument, we have computed the adsorption energy of MeSH on the more likely experimental scenario, that is, the reconstructed case. The reaction is found to be exothermic by −9.8 kcal/mol. and this brings down the total reaction energy into exothermic region by −9.6 kcal/mol (see Fig. 3; note here that the adatom formation that was estimated to be exothermic by −3.3 kcal/mol from our periodic DFT study [73] has not been taken into account in this energetics equation).

The transition state modeling performed so far releases hydrogen atom, which upon recombination with hydrogen produces H_2 molecule as it is also evident from the experiments. In an ordered $(\sqrt{3} \times \sqrt{3})$R30° SAM arrangement, since the two methylthiols are close to each

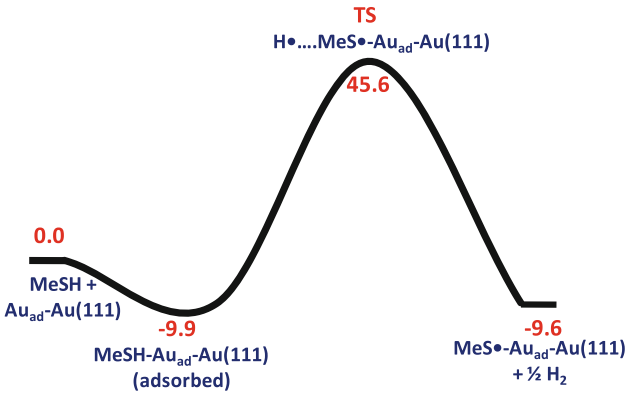

Fig. 3 Computed PES for the reaction of MeSH on Au(111)

other, it is likely that the cleavage of the two methylthiols S–H bonds and formation of H_2 can occur simultaneously through a concerted transition state. This is especially true for high-coverage regime where the methylthiols arrange with one another with a short intermolecular distance. An attempt to compute such transition state was successful and yields a very low barrier height of 20.7 kcal/mol. Consequently, now the reaction energy falls in the exothermic regime by −14.9 kcal/mol. The optimized structure of the transition state is shown in Fig. 1c. At the transition state, two MeSH groups are in *trans* configuration [130] with a S–S distance of 4.05 Å. The S–H bonds are elongated to 1.43 Å while the H···H interaction is at 1.20 Å. Although this co-operative transition state is likely to be the realistic model for the S–H cleavage, since a very close sulfur–sulfur interaction is mandatory for this transition state to occur, it is very likely that this happens in high-coverage regime. On the other hand, in low coverage regime, the single molecule TS presented before could be the most likely.

These results clearly illustrate that the dissociation of the S–H bond is homolytic in nature without a prohibitive kinetic barrier and is also likely to be aided by the defects on the surface. A co-operative mechanism is instead expected when short intermolecular interactions, that is, high coverage, are present.

3.2 Dimethylsulfide (DMS)

As a natural extension to methylthiols, we have considered dimethylsulfide adsorption on Au(111). There are several experimental reports on the dimethylsulfide adsorption on Au(111) [100–104]. In this case, a homolytic S–C cleavage is expected as the resulting radical species is likely to adsorb firmly on the surface. This assumption is supported by experimental bond dissociation energy (BDE) of the S–C bond in DMS, which is much lower than the S–H bond in the methylthiols. Additionally, there is also convincing spectroscopic evidence where S–C cleavage has been observed for some alkylthiols on Ag surface [131–137]. Considering these facts, the CH_3S-CH_3 cleavage transition state has been modeled and computed. The activation and reaction energies are given in Table 3, while selected structural parameters of the optimized structure are given in Table 4. The optimized geometry of adsorption of DMS on clean and reconstructed surface is presented in Fig. 4. The barrier for S–C bond cleavage after the adsorption of DMS on Au(111) is found to be 69.6 kcal/mol on clean surface, and the reaction is found to be endothermic by 3.9 kcal/mol. The S–C bond length is found to 1.89 Å in the reactant while it elongates in the transition state up to 3.55 Å (Fig. 4a). A very long S–C bond in transition state indicates a product-like transition state. Spin densities of −0.22 on the sulfur atom and −1.12 and 0.01 on the two carbon atoms are observed. Such scenario clearly shows that the dissociation of S–C bond occurs homolytically.

In the presence of gold adatoms, the barrier gets reduced from 69.6 to 55.6 kcal/mol while the reaction becomes exothermic with a reaction energy of −3.6 kcal/mol. As in the methyl thiols, the cleavage is aided in the presence of Au adatom. In the reconstructed surface, the S–C bond elongates from 1.90 to 4.49 Å and the computed spin densities is almost similar to that of S–C bond cleavage occurs in the clean surface. A lower BDE for the dimethylsulfide compared to methylthiols indicates that the S–C cleavage is perhaps more facile than S–H bond cleavage, and this is reflected in the computed barrier heights (72.6 vs. 55.6 kcal/mol) [55, 103].

3.3 Dimethyldisulfide (DMDS)

A few thiolated species has been chosen to model the kinetics where the cleavage has been clearly envisaged with both experimental and theoretical studies. On this account, dimethyldisulfide takes the prime place as there are numerous experimental and theoretical studies on its adsorption on Au(111). The transition state geometry of dissociation of DMDS on clean and reconstructed surface is presented in Fig. 5. Activation and reaction energies and

Table 3 Activation and reaction energies of the dissociation of various alkylthiol and their alternatives on clean and reconstructed surface

	Partial optimization			
	Clean surface		Constructed surface	
	$\Delta G^{\#}$	ΔG_r	$\Delta G^{\#}$	ΔG_r
CH_3–S–CH_3	69.6	3.9	55.6	−3.6
CH_3–S–S–CH_3	17.47	−4.2	23.7	−2.4
CH_3–S–OAc	–	–	13.9	7.2
CH_3–S–CN	46.7	–	6.4	–

Table 4 Selected structural parameters of adsorption and dissociation of DMS, thioacetate, thiocyanate on clean and reconstructed Au(111) surface along with spin densities on S and H atoms

	Spin densities		Structural parameters		
	S	C	S–C	Au–S	Au–S–C
DMS					
Popt					
R	0.33	−0.66	1.89	3.17	107.4
TS	−0.22	1.12	3.55	2.71	127.7
$Popt_{Add}$					
R	0.39	−0.63	1.90	2.50	100.2
TS	−0.22	1.13	4.49	2.39	71.1
Thioacetate					
$Popt_{Add}$					
R	0.39	−0.63	1.99	2.77	96.9
TS	0.0	0.0	2.13	2.78	91.1
Thiocyanate					
Popt					
R	0.0	0.0	1.75	3.52	91.9
TS	−0.44	0.22	2.43	2.84	115.9
$Popt_{Add}$					
R	0.0 (0.58)	0.0 (−0.07)	1.76	2.56	99.5
TS	0.44 (0.59)	0.0 (−0.02)	4.42Å	2.42	104.0

structural parameters of adsorption of DMDS on clean and reconstructed gold surface are given in Tables 3 and 5. The barrier for dissociation of DMDS on the Au(111) after the adsorption is found to 17.5 kcal/mol, and the reaction is exothermic by −4.2 kcal/mol. Combined low-energy electron diffraction, Auger electron spectroscopy, X-ray photoelectron spectroscopy, and line of sight mass spectrometry have been used to study the adsorption and desorption of DMDS on Au(111). According to these works, the S–S bond clearly cleaves on the surface and the estimated barrier height is to be in the range of 14.6–15.3 kcal/mol [105].

In the dissociation transition state, S–S bond length is 4.28 Å while during adsorption S–S bond length is 2.27 Å (Fig. 3b). In the dissociation transition state, DMDS molecule shows significant spin densities on the two S atoms ensuring that dissociation of DMDS occur homolytically. The computed structure and barrier heights are in good agreement with earlier experimental and theoretical observations [105].

3.4 Thiocyanates

Experimental studies reveal that thiocyanates chemisorb on gold surface after the cleavage of S–CN bond and, moreover, high-quality SAM is formed after the occurrence of surface-mediated reduction of thiocyanates on Au(111) surface [82]. In order to find out the kind of cleavage and whether surface-mediated reduction or homolytic cleavage occurs during the dissociation of S–C bond of thioacetate, we have modeled the transition state for dissociation of S–C(CN) bond of thioacetates on the clean and reconstructed Au(111) surface (see Tables 3, 4; Fig. 6). The energy barrier for dissociation of thiocyanates on the clean surface is 46.7 kcal/mol. In the dissociation transition state, Au–S and S–C bond distance is found to be 2.84 and 4.32 Å. During adsorption, Au–S and S–C bond distance is found to be 3.52 and 1.75 Å. In the dissociation transition state, thiocyanates has −0.44 and 0.22 on the sulfur and carbon atoms. This clearly shows the homolytic cleavage occurs during the dissociation of thiocyanates on the clean Au(111) surface. The barrier for the dissociation of thiocyanate on the reconstructed surface is very low with just 6.4 kcal/mol and reveals that thiocyanates among other studies have the lowest kinetic requirement for the cleavage to occur and this explains more regular ordered SAMs formed in general with thiocyanates [82–84].

3.5 Thioacetates

Thioacetates are routinely used in the preparation of SAMs as they serve as best protecting groups from unwarranted reactions to occur. Moreover, it has been shown that experimentally the thioacetates undergo spontaneous deprotection upon adsorption, leading to radical thiols to be adsorbed on the surface [91, 92]. This approach has been

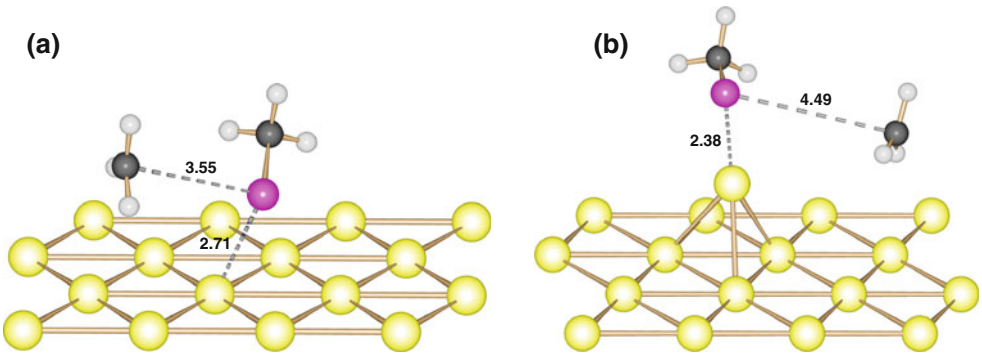

Fig. 4 Dissociation transition of DMS on clean and reconstructed surface (S = pink, H = white, C = gray, Au = yellow)

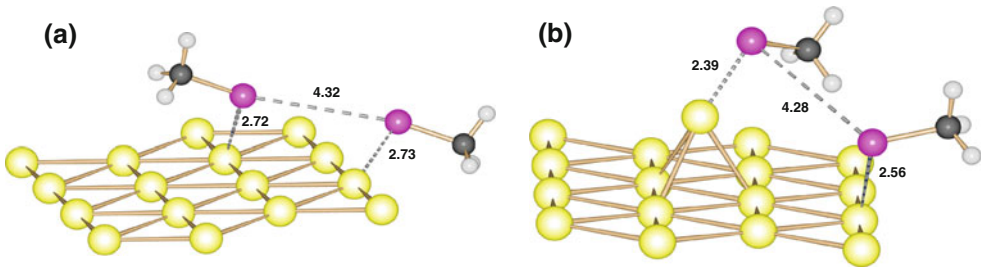

Fig. 5 Dissociation transition of DMDS on clean and reconstructed surface (S = pink, H = white, C = gray, Au = yellow)

Table 5 Activation and reaction energies of the dissociation of DMDS on clean and reconstructed Au(111) surface

	Spin densities		Structural parameters					
	S	S	S–S	Au–S	Au–S_1–S_2	Au–S_2–S_1	Au–S_1–C	Au–S_2–C
Popt								
R	0.0	0.0	2.25	3.34	103.0	70.7	153.9	104.5
TS	0.02	0.15	4.32	2.73	85.9	92.1	83.3	101.9
$Popt_{Add}$								
R	0.0	0.0	2.27	2.50	104.5		99.5	
TS	0.49	0.20	4.28	2.39	84.7	101.4	99.4	90.9

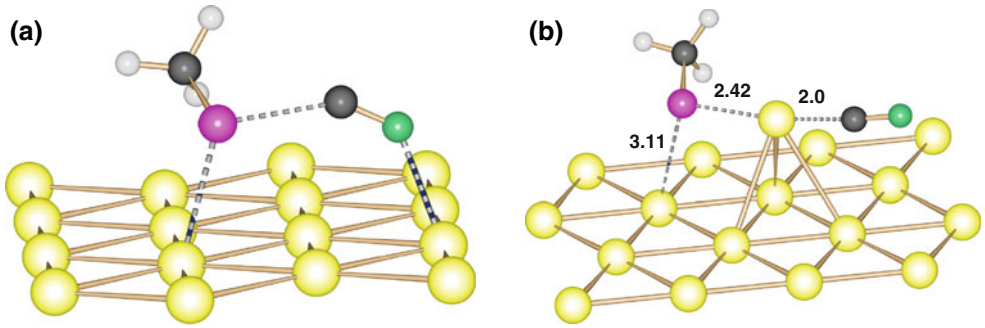

Fig. 6 Dissociation transition of thiocyanate on the clean and reconstructed surface (S = pink, H = white, C = gray, Au = yellow, N = green)

successively used for the synthesis of SAMs of different nature [92]. An earlier experimental study clearly suggests that dissociation of long chain alkylethioactetates after the adsorption occurs through a polar transition states, and the long chain alkylthioacetates adsorb slower than the corresponding thiols. In order to find out which mode of cleavage occurs during the dissociation of S–C bond of thioacetate, we have modeled the transition state for dissociation of S–C bond of thioacetates on the most likely reconstructed surface (Fig. 7). The barrier for dissociation of S–C bond of thioacetate on Au(111) is found to be 13.9 kcal/mol, and the reaction is found to be endothermic by 7.2 kcal/mol. Very small spin densities on the sulfur and carbon atoms in the transition state have been found. On the other hand, significant Mulliken charges on these atoms reveal that the transition state is polar in nature.

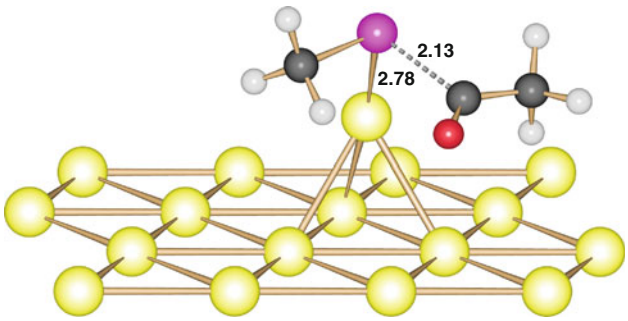

Fig. 7 Dissociation transition of thioacetate on reconstructed surface (S = pink, H = white, C = gray, Au = yellow, Red = Oxygen)

On the other hand, the stabilized products are homolytically cleaved.

Our computed dissociation transitions state and energetic are in good agreement with earlier experimental

observations [88, 91, 92]. Our calculations seem therefore to suggest a homolytic cleavage assisted by a polarized transition state.

4 Conclusions

The present study aims to probe the kinetic and thermodynamic aspects of the S–X (X = Me, S, Acetyl, CN) cleavage of various alkylthiols during the adsorption on clean and reconstructed Au(111) surface using DFT methods. The transition state for each species has been modeled on a single layer of gold atoms, and the barrier height and the reaction energies were then computed. The following points emerge from our calculations, and some of these conclusion are also supported by independent experiments,:

1. The cleavage of S–H bond in MeSH occurs homolytically on clean and reconstructed Au surface. The homolytic cleavage of S–H bond is found to have lower barrier height on reconstructed surface, that is, in the presence of gold adatoms. This result reveals that the adatom is supposed to aid the cleavage of S–H bonds resulting in stable and ordered SAMs. Additionally, our calculations show that the cleaved hydrogen atoms can recombine and leave as H_2, as also experimentally detected.
2. In this framework, we have shown the intermolecular distances play an important role in the S–H cleavage kinetics. Short inter-thiols distances favor a concerted transition state with a lower activation energy than the one found for an isolated thiol molecule on gold. This leads us to conclude that, at least in high-coverage regime, a cooperative cleavage of the S–H bond with a spontaneous release of the H_2 is expected.
3. Our calculations suggest that the S–C bond in the DMS is also likely to cleave homolytically. Such suggestion is supported by a lower activation energy than the one found for the S–H cleavage of the methylthiol.
4. The computed activation free energy for the S–S bond cleavage of the DMDS is found to be in agreement with the experimentally reported values. The computed barrier height reveals that the S–S cleavage rates are likely to be faster than the S–H and S–C cleavage of the MeSH and DMS, respectively.
5. Among the various substituted alkylthiols, the following order is found for the cleavage kinetics: CH_3–S–CN > CH_3–S–OAc > CH_3–S–S–CH_3 > CH_3–S–CH_3 > CH_3–S–H. This clearly illustrates the role of electronegativity on the homolytic cleavage of alkylthiols on reconstructed gold surface.

Acknowledgments GR would like to acknowledge the financial support from the Government of India through Department of Science and Technology (SR/S1/IC-41/2010) and generous computational resources from Indian Institute of Technology Bombay. MJ thanks Indian Institute of Technology Bombay for financial support through Institute Post Doctoral Fellowship. FT acknowledges FP7-STREP: MOLSPINQIP–ICT-211284 'Molecular Spin Clusters for Quantum Information Processing', ERC-2010-AdG—no 267746 MolNaMaS—'Molecular Nanomagnets at Surfaces: Novel Phenomena for Spin-based Technologies', and PRIN 2008—FZK5AC, 'Strutture molecolari e nanocristalline con funzionalità magnetiche, foto-magnetiche e foto-emettitrici e loro organizzazione su superfici, in film polimerici o in sol–gel'.

References

1. Ulman A (1996) Chem Rev 96:1533
2. Bumm LA, Arnold JJ, Cygan MT, Dunbar TD, Burgin TP, Jones L, Allara DL, Tour JM, Weiss PS (1996) Science 271:1705
3. Poirier GE (1997) Chem Rev 97:1117
4. Reed MA, Zhou C, Muller CJ, Burgin TP, Tour JM (1997) Science 278:252
5. Ulman A (2001) Acc Chem Res 34:855
6. Nitzan A, Ratner MA (2003) Science 300:1384
7. Love JC, Estroff LA, Kriebel JK, Nuzzo RG, Whitesides GM (2005) Chem Rev 105:1103
8. Heimel G, Romaner L, Zojer E, Bredas JL (2008) Acc Chem Res 41:721
9. Chen W, Wee ATS (2009) J Electron Spectros Relat Phenomena 172:54
10. Kumar A, Abbott NL, Biebuyck HA, Enoc K, Whitesides GM (1995) Acc Chem Res 28:219
11. Houston JE, Kim IH (2002) Acc Chem Res 35:547
12. Woodruff DP (2006) Phys Chem Chem Phys 10:7211
13. Vericat C, Vela ME, Benitez GA, Martin Gago JA, Torrelles X, Salvarezza RC (2006) J Phys Condens Matter 18:867
14. Dubois LH, Nuzzo RG (1992) Ann Rev Phys Chem 43:437
15. Kramer S, Fuierer RR, Gorman CB (2003) Chem Rev 103:4367
16. Chidsey CED, Liu G-Y, Rowntree YP, Scoles G (1989) J Chem Phys 91:4421
17. Alves CA, Smith EL, Porter MD (1992) J Am Chem Soc 114:1222
18. Poirier GE, Tarlov MJ, Rushneier HE (1994) Langmuir 10:3383
19. Fenter P, Eisenberger P, Liang KS (1993) Phys Rev Lett 70:2447
20. Camillone N, Chidsey CED, Liu G-Y, Scoles G (1993) J Phys Chem 98:3503
21. Poirier GE, Tarlov MJ (1994) Langmuir 10:2859
22. Poitier GE, Pylant ED (1996) Science 272:1145
23. Sellers H, Ulman A, Shnidman Y, Eilers JE (1993) J Am Chem Soc 115:9389
24. Gronbeck H, Curioni A, Andreoni W (2000) J Am Chem Soc 122:3839
25. Yourdshahyan Y, Zhang HK, Rappe AM (2001) Phys Rev B 63:81405
26. Tachibana M, Yoshizawa K, Ogawa A, Fujimoto H, Hofmann R (2002) J Phys Chem B 106:12727
27. Hayashi T, Morikawa Y, Nozoye H (2001) J Chem Phys 114:7615
28. Vargas C, Giannozzi P, Selloni A, Scoles G (2001) J Phys Chem B 105:9509
29. Gottschalck J, Hammer B (2002) J Chem Phys 116:784

30. Molina ML, Hammer B (2002) Chem Phys Lett 360:264
31. Morikawa Y, Liew CC, Nozoye H (2002) Surf Sci 514:389
32. Roper MG, Skegg MP, Fisher CJ, Lee JJ, Dhank VR, Woodruff DP, Jones RG (2004) Chem Phys Lett 389:87
33. Kondoh H, Iwasaki M, Shimada T, Amemiya K, Yokoyama T, Ohta T, Shimomura M, Kono S (2003) Phys Rev Lett 90:066102
34. Yu M, Bovet N, Satterley CJ, Bengió S, Lovelock KRJ, Milligan PK, Jones RG, Woodruff DP, Dhanak V (2006) Phys Rev Lett 97:166102
35. Maksymovych P, Sorescu DC, Dougherty D, Yates TY Jr (2005) J Phys Chem B 109:22463
36. Maksymovych P, Sorescu DC, Yates TY Jr (2006) Phys Rev Lett 97:146103
37. Grönbeck H, Häkkinen H (2007) J Phys Chem B 111:3325
38. Mazzarello R, Cossaro A, Verdini A, Rousseau R, Casalis L, Danisman MF, Floreano L, Scandolo S, Morgante A, Scoles G (2007) Phys Rev Lett 98:016102
39. Nogoya A, Morikawa Y (2007) J Chem Phys 19:365245
40. Wang J-G, Selloni A (2007) J Phys Chem C 111:12149
41. Cossaro A, Mazzarello R, Rousseau R, Casalis L, Verdini A, Kohlmeyer A, Floreano L, Scandolo S, Morgante A, Klein ML, Scoles G (2008) Science 321:943
42. Maksymovych P, Yates JT (2008) J Am Chem Soc 130:7518
43. Carro P, Salvarezza R, Torres D, Illas F (2008) J Phys Chem C 112:19121
44. Kautz NA, Kandel SA (2008) J Am Chem Soc 130:6908
45. Voznyy O, Dubowski JJ (2009) Langmuir 25:7353
46. Groenbeck H, Haekkinen H, Whetten RL (2008) J Phys Chem C 112:15940
47. Jiang D (2009) Chem Phys Lett 477:90
48. Franke A, Pehlke E (2009) Phys Rev B 79:235441
49. Jiang D, Dai S (2009) J Phys Chem C 113:3763
50. Wang J, Selloni A (2009) J Phys Chem C 113:3763
51. Chaudhuri A, Lerotholi TJ, Jackson DC, Woodruff DP, Jones RG (2009) Phys Rev B 79:195439
52. Chaudhuri A, Lerotholi TJ, Jackson DC, Woodruff DP, Dhanak V (2009) Phy Rev Lett 102:126101
53. Torres E, Blumenau AT, Biedermann PU (2009) Phy Rev B: Condens Matter 79:075440
54. Voznyy O, Dubowski JJ, Yates JT, Maksymovych P (2009) J Am Chem Soc 113:12989
55. Schlenoff JB, Li M, Ly H (1995) J Am Chem Soc 117:12528
56. Walczak MW, Chung C, Stole SM, Widrig CA, Porter MD (1991) J Am Chem Soc 113:2370
57. Brust M, Walker M, Bethell D, Schiffrin DJ, Whyman R (1994) J Chem Soc, Chem Commun 801
58. Thomas RC, Sun L, Crooks M (1991) Langmuir 7:620
59. Chailapakul O, Sun L, Xu C, Crooks M (1993) J Am Chem Soc 115:12459
60. Porter MD, Bright TB, Allara DL, Chidsey CED (1987) J Am Chem Soc 109:3559
61. Nuzzo RG, Fusco FA, Allara DL (1987) J Am Chem Soc 109:2358
62. Bain CD, Biebuyck HA, Whitesides GM (1989) Langmuir 5:723
63. Nuzzo RG, Zegarski BR, Dubois LH (1987) J Am Chem Soc 109:733
64. Nuzzo RG, Dubois LH, Allara DL (1990) J Am Chem Soc 112:558
65. Li Y, Huang J, McIver RT Jr, Hemminger JC (1992) J Am Chem Soc 114:2428
66. Widrig CA, Chung C, Porter MD (1991) J Electroanal Chem 310:335
67. Bryant MA, Pemberton JE (1991) J Am Chem Soc 113:3630
68. Bryant MA, Pemberton JE (1991) J Am Chem Soc 113:8284
69. Kankate L, Turchanin A, Gölzhäauser A (2009) Langmuir 25: 10435
70. Tielens F, Santos E (2010) J Phys Chem C 114:9444
71. RzezinickaII, Lee JS, Maksymovych P, Yates JT (2005) J Phys Chem B 109:15992
72. Hasan M, Bethell D, Brust M (2002) J Am Chem Soc 124:1132
73. Rajaraman G, Caneschi A, Gatteschi D, Totti F (2011) Phys Chem Chem Phys 13:3886
74. Beulen MWJ, Bugler J, Lammerink B, Geurts FAJ, Biemond EMEF, Van Leerdam KGC, Van Veggel FCJM, Engbersen JFJ, Reinhoudt DN (1998) Langmuir 14:6424
75. Friggeri A, Schoenherr H, van Manen H-J, Huisman B-H, Vancso GJ, Huskens J, van Veggel FCJM, Reinhoudt DN (2000) Langmuir 16:7757
76. Faull JD, Gupta VK (2002) Langmuir 18:6584
77. Liebau M, Janssen HM, Inoue K, Shinkai S, Huskens J, Si-jbesma RP, Meijer EW, Reinhoudt DN (2002) Langmuir 18:674
78. Yamada T, Sekine R, Sawaguchi T (2000) J Chem Phys 113:1217
79. Houmam A, Hamed EM, Hapiot P, Motto JM, Schwan AL (2003) J Am Chem Soc 125:12676
80. Houmam A, Hamed EM, Still IWJ (2003) J Am Chem Soc 125: 7258
81. Kordis J, Gingerich KA, Seyse RJ (1974) J Chem Phys 61:5114
82. Coi Y, Jeong Y, Chung H, Tto E, Hara M, Noh J (2008) Langmuir 24:91
83. Dietz O, Rayon VM, Frenking G (2003) Inorg Chem 42:4977
84. Ciszek JW, Stewart MP, Tour JM (2004) J Am Chem Soc 126: 13172
85. Singh A, Dahanayaka DH, Biswas A, Bumm L, Haltermanm RL (2010) Langmuir 26:13221
86. Tour JM, Jones LII, Pearson DL, Lamba JJS, Burgin TP, Whitesides GM, Allara DL, Parikh AN, Atre SV (1995) J Am Chem Soc 117:9529
87. Cai L, Yao Y, Yang J, Price DW, Tour JM (2002) Chem Mater 14:2905
88. Stapleton JJ, Harder P, Daniel TA, Reinard MD, Yao Y, Price DW, Tour JM, Allara DL (2003) Langmuir 19:8245
89. Park T, Kang H, Choi I, Chung H, Ito E, Hara M, Noh J (2009) Bull Korean Chem Soc 30:441
90. Kang Y, Won D, Kim S, Seo K, Choi H, Lee G, Noh Z, Lee T, Lee C (2004) Mater Sci Eng C 24:43
91. Béthencourt MI, Srisombat L-O, Chinwangso P, Lee TR (2009) Langmuir 25:1265
92. Rodriguez-Douton MJ, Mannini M, Armelao L, Barra A-L, Tancini E, Sessoli R, Cornia A (2011) Chem Commun 47:1467
93. Park T, Kang H, Kim Y, Lee S, Noh J (2011) Bull Korean Chem Soc 32:39
94. Noh J, Murase T, Nakajima K, Lee H, Hara M (2000) J Phys Chem B 104:7411
95. Jung C, Dannenberger O, Xu Y, Buck M, Grunze M (1998) Langmuir 14:1103
96. Lee H, He Z, Hussey CL, Mattern DL (1998) Chem Mater 10:4148
97. Leavy MC, Bhattacharyya S, Cleland WE Jr, Hussey CL (1999) Langmuir 15:6582
98. Takiguchi H, Sato K, Ishida T, Abe K, Yase K, Tamada K (2000) Langmuir 16:1703
99. Noh J, Kato HS, Kawai M, Hara M (2002) J Phys Chem B 106:13268
100. Beulen MWJ, Huisman B-H, van der Heijden PA, van Veggel FCJM, Simons MG, Biemond EMEF, de Lange PJ, Reinhoudt DN (1996) Langmuir 12:6170
101. Noh J, Nakamura F, Kim J, Lee H, Hara M (2002) Mol Cryst Liq Cryst 377:165
102. Schoenherr H, Vancso GJ, Huisman B-H, Van Veggel FCJM, Reinhoudt DN (1999) Langmuir 15:5541
103. Zhong C-J, Porter MD (1994) J Am Chem Soc 116:11616

104. Zhong C-J, Brush RC, Anderegg J, Porter MD (1999) Langmuir 15:518
105. Roper MG, Jones RG (2008) Phys Chem Chem Phys 10:1336
106. Cometto FP, Macagno VA, Paredes-Olivera P, Patrito EM, Ascolani H, Zampieri G (2010) J Phys Chem C 114:10183
107. Khayankarn O, Pearson RA, Verghese N, Shafi A (2005) J Adhes 81:941
108. Béthencourt MI, Barriet D, Frangi NM, Lee TR (2005) J Adhes 81:1031
109. Colorado R Jr, Lee TR (2003) Langmuir 19:3288
110. Zhang X, Chabal YJ, Christman SB, Chaban EE, Garfunkel E (2001) J Vac Sci Technol A 19:1725
111. Cai L, Yao Y, Yang J, Price DW, Tour JM (2002) Chem Mater 14:2905
112. Béthencourt MI, Srisombat L-o, Chinwangso P, Lee TR (2009) Langmuir 25:1265
113. Bencini A, Rajaraman G, Totti F, Tusa M (2009) Superlattices Microstruct 46:4
114. Rajaraman G, Caneschi A, Gatteschi D, Totti F (2010) J Mat Chem 20:10747
115. Jaguar 7.0, Schrödinger, Portland, OR 97204
116. Becke AD (1993) J Chem Phys 98:5648
117. Stephens PJ, Devlin FJ, Chabalowski CS, Frisch MJ (1994) J Phys Chem 98:11623
118. Hay PJ, Wadt WR (1985) J Chem Phys 82:270
119. Hay PJ, Wadt WR (1985) J Chem Phys 82:284
120. Hay PJ, Wadt WR (1985) J Chem Phys 82:299
121. Hariharan PC, Pople JA (1973) Theor Chim Acta 28:213
122. Francl MM, Petro WJ, Hehre WJ, Binkley JS, Gordon MS, DeFrees DJ, Pople JA (1982) J Chem Phys 77:3654
123. Rassolov V, Pople JA, Ratner M, Windus TL (1998) J Chem Phys 109:1223
124. Schaftenaar G, Noordik JH (2000) Molden: a pre- and post-processing program for molecular and electronic structures. J Comput Aided Mol Design 14:1
125. Mundy CJ, Mohamed F, Schiffman F, Tabacchi G, Forbert H, Kuo W, Hutter J, Krack M, Iannuzzi M, McGrath M, Guidon M, Kuehne TD, Laino T, VandeVondele J, Weber V (2000) CP2K software package, http://cp2k.berlios.de
126. VandeVondele J, Krack M, Mohamed F, Parrinello M, Chassaing T, Hutter J (2005) Comput Phys Commun 167:103
127. Lippert G, Hutter J, Parrinello M (1997) Mol Phys 92:477
128. Lippert G, Hutter J, Parrinello M (1999) Theor Chem Acc 103:124
129. Kong B, Kim Y, Choi SI (2008) Bull Korean Chem Soc 29:1843
130. Cometto FP, Macagno VA, Paredes-Olivera P, Patrito EM, Ascolani H, Zampieri, G (2010) J Phys Chem C 114:10183
131. Kim KL, Lee SJ, Kim K (2004) J Phys Chem B 108:9216
132. Baadji N, Piacenza M, Tugsuz T, Della SF, Maruccio G, Sanvito S (2009) Nat Mater 8:813
133. Zulczewski G, Sanvito S, Coey M (2009) Nat Mater 8:693
134. Zhang R, Ma G, Li R, Qian Z, Shen Z, Zhao X, Hou S, Sanvito S (2009) J Phys Condens Matter 21:335301
135. Giusti A, Charron G, Mazerat S, Compain J-D, Mialane P, Dolbecq A, Riviere E, Wernsdorfer W, Ngo B, Keita B, Nadjo L, Filoramo A, Bourgoin J-P, Mallah T (2009) Angew Chem Int Ed 48:4949
136. Wernsdorfer W (2009) Nat Nanotechnol 4:145
137. Bogani L, Wernsdorfer W (2008) Nat Mater 7:179